Thermochimica Acta, 115 (1987) 45–55
Elsevier Science Publishers B.V., Amsterdam – Printed in The Netherlands

THERMAL STUDIES ON PURINE COMPLEXES. XIII. BROMOCOMPLEXES OF SOME ALKYLXANTHINE DERIVATIVES

M.I. MORENO-VIDA, E. COLACIO-RODRÍGUEZ, M.N. MORENO-CARRETERO, J. RUIZ-SÁNCHEZ and J.M. SALAS-PEREGRÍN *

Department of Inorganic Chemistry, University of Granada, 18071 Granada (Spain)

(Received 16 September 1986)

ABSTRACT

Palladium(II) ions react in aqueous and strong hydrobromic acid media with xanthine derivatives to give compounds with the general simplified formulae $PdBr_2(LH)_2$ and $[PdBr_4][LH_2]_2$ or $[PdBr_3][LH_2]\cdot xH_2O$ (LH = alkylxanthine derivative), respectively. The thermal behaviour of these complexes has been determined from their TG, DTG and DSC curves.

INTRODUCTION

It is well known that metal ions play an important role in the biochemistry of nucleic acids [1]; for example, the transfer of ATP phosphoryl, which is an enzymatic process essentially, requires the presence of metal ions. The discovery of the antitumour activity of *cis*-$[Pt(NH_3)_2Cl_2]$ [2,3] has created much interest in the synthesis of complexes of the *cis*-$[M(L)_2X_2]$ type (where M = Pt and Pd) which could be used against a variety of tumours. Studies on the thermal behaviour of metal complexes with purine and pyrimidine derivatives as ligands are still scarce in the literature, especially compared with those related to other techniques [4–7].

In this paper, continuing the thermal studies on some metal complexes of xanthine derivatives [8–11], we report the synthesis and thermal behaviour of several Pd(II) complexes of the general formulae $PdBr_2(LH)_2$, $[PdBr_4][LH_2]_2$ and $[PdBr_3][LH_2]\cdot xH_2O$. The different ligands used in this work are shown in Scheme 1.

---

* To whom all correspondence should be addressed.

0040-6031/87/$03.50

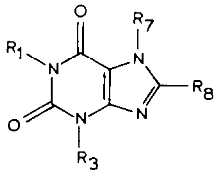

R_1	R_3	R_7	R_8	LH
H	H	H	Et	8EH
Me	H	H	Et	1MEH
H	Me	Me	H	TBH
H	Me	H	Me	DMH
Me	Me	H	H	TFH
Me	Me	Me	H	CF
Me	Me	H	Me	TMH
Me	Me	H	Et	ETH
Me	Me	H	Pr	PRH
Me	Me	H	iPr	IPH
Me	Me	H	Pen	PH

Scheme 1

EXPERIMENTAL

Theobromine (TBH), theophylline (TFH) and caffeine (CF) were purchased from Carlo Erba; the other purine bases were synthesized by us, following Speer's method [12]. After recrystallization using water, the different xanthine derivatives were obtained as white crystalline needles. All the chemicals used in this work were of analytical reagent grade.

METHODS

Microanalyses of C, H and N were carried out in the Instituto de Química Bio-Orgânica (C.S.I.C.) Barcelona. Palladium and water were determined gravimetrically, using a Mettler TG-50 thermobalance. Infrared (IR) spectra were recorded on a Perkin-Elmer 983-G spectrophotometer using KBr and polyethylene pellets.

Thermogravimetric (TG) and differential scanning calorimetry (DSC) curves were recorded on a Mettler TA-3000 system with a Mettler TG-50 thermobalance and a Mettler DSC-20 differential scanning calorimeter. TG diagrams were realized in a dynamic atmosphere of pure air (100 ml min^{-1}), at a heating rate of 10 °C min^{-1}, using samples varying in weight from 6.72 to 22.04 mg. DSC curves were obtained in a static atmosphere of air with the samples varying in weight from 1.08 to 4.03 mg, at the same heating rate as for the TG plots.

PREPARATION OF THE COMPLEXES

Complexes of the type $PdBr_2(LH)_2$ were obtained by mixing aqueous solutions containing the corresponding xanthine derivative and $Na_2[PdBr_4]$

TABLE 1

Analytical data of the isolated compounds (%) [a]

Compound	C	H	N	Pd
$PdBr_2(8EH)_2$	26.82	2.47	17.04	17.21
	(26.83)	(2.56)	(17.89)	(16.99)
$PdBr_2(1MEH)_2 \cdot H_2O$	29.03	3.26	16.67	14.60
	(28.56)	(3.27)	(16.66)	(15.83)
$PdBr_2(TBH)_2$	27.10	2.33	17.57	17.03
	(26.83)	(2.56)	(17.89)	(16.99)
$PdBr_2(DMH)_2 \cdot 3H_2O$	24.64	3.12	16.04	16.16
	(24.70)	(3.23)	(16.47)	(15.64)
$PdBr_2(TFH)_2 \cdot H_2O$	26.97	2.82	17.29	16.87
	(26.08)	(2.79)	(17.39)	(16.52)
$PdBr_2(CF)_2$	29.53	2.95	16.73	16.20
	(29.35)	(3.06)	(17.12)	(16.26)
$PdBr_2(TMH)_2 \cdot 2H_2O$	28.08	3.26	16.30	15.48
	(27.81)	(3.48)	(16.23)	(15.42)
$PdBr_2(ETH)_2 \cdot 2H_2O$	30.11	3.65	15.01	15.03
	(30.08)	(3.90)	(15.59)	(14.81)
$PdBr_2(PRH)_2$	33.41	3.93	14.94	15.67
	(33.79)	(3.94)	(15.77)	(14.98)
$PdBr_2(IPH)_2$	33.72	3.99	15.25	15.31
	(33.79)	(3.94)	(15.77)	(14.98)
$PdBr_2(PH)_2$	37.70	4.70	14.54	14.06
	(37.59)	(4.70)	(14.62)	(13.89)
$PdBr_4(TBH_2)_2$	21.68	2.23	13.83	12.90
	(21.32)	(2.28)	(14.21)	(13.50)
$PdBr_4(TFH_2)_2$	21.44	2.26	13.93	13.26
	(21.32)	(2.28)	(14.21)	(13.50)
$PdBr_3(CFH) \cdot 7H_2O$	14.18	2.84	7.62	16.66
	(14.39)	(3.74)	(8.39)	(15.95)
$PdBr_3(TMH_2) \cdot H_2O$	16.70	2.18	9.71	18.49
	(17.17)	(2.32)	(10.01)	(19.03)
$PdBr_3(ETH_2) \cdot H_2O$	18.71	2.74	9.15	18.37
	(18.84)	(2.62)	(9.77)	(18.56)
$PdBr_3(PRH_2) \cdot 2H_2O$	19.91	3.02	8.90	17.19
	(19.83)	(3.14)	(9.25)	(17.58)
$PdBr_3(IPH_2) \cdot 2H_2O$	20.32	3.07	8.91	17.39
	(19.83)	(3.14)	(9.25)	(17.58)
$PdBr_3(PH_2) \cdot H_2O$	23.99	3.36	8.97	16.56
	(23.41)	(3.41)	(9.10)	(17.30)

[a] Calculated values are given in parentheses.

in a 2/1 molar ratio. After a few minutes, a yellow powder appeared in all cases. This was filtered off, washed consecutively with ethanol and diethylether and air-dried.

Compounds of $[PdBr_4][LH_2]_2$ and $[PdBr_3][LH_2] \cdot xH_2O$ types were prepared following a previously described method [13]. These compounds were isolated as red crystals.

The chemical analyses of isolated compounds are collected in Table 1.

RESULTS AND DISCUSSION

Yellow complexes

The most significant IR bands for complexes of the type $PdBr_2(LH)_2$ are given in Table 2. From a comparative study carried out between the positions of these bands and those corresponding to free ligands [10,14,15], it is possible to observe a shift to lower wavenumber of the bands corresponding to $\nu(C_2{=}O)$ and $\nu(C{=}C) + \nu(C{=}N)$ and a shift to a higher wavenumber of the $\nu(C_6{=}O)$ band. The position of these bands and the magnetic studies carried out on these complexes (all are diamagnetic) suggest that they are all mononuclear square-planar molecules containing two xanthine derivatives bound in monodentate form through N9. On the other hand, the presence of only one band assignable to the stretching vibration $\nu(Pd{-}N)$ and/or $\nu(Pd{-}Br)$ is consistent with a *trans* geometry in these complexes. This coordination mode has also been observed for the analogous $PdCl_2(LH)_2$ complexes [9].

The thermal behaviour of $PdBr_2(LH)_2$ complexes is very similar. All of them show two principal processes: (i) dehalogenation, and (ii) decomposition. Furthermore, complexes of 1MEH, DMH, TFH, TMH and ETH also show a dehydration process in the 50–150 ° C temperature range.

Figure 1 shows TG and DSC curves for the complexes $PdBr_2(TMH)_2 \cdot 2H_2O$ and $PdBr_2(PRH)_2$. The most interesting TG and DSC data for these complexes are given in Table 3.

Dehydration processes appear as one or two endothermic effects in the corresponding DSC curve. For $PdBr_2(TMH)_2 \cdot 2H_2O$, the presence of two overlapping endothermic effects at 70 and 85 ° C indicates the non-equivalence of the molecules of water, probably due to the different interactions of these water molecules with the xanthine derivative rings. The average enthalpy value calculated for the dehydration process of $PdBr_2(TMH)_2 \cdot 2H_2O$ is practically the same as that calculated for $PdCl_2(XH)_2 \cdot 2H_2O$ (where XH = xanthine) [16].

Once dehydrated, anhydrous complexes are thermally stable up to 275 ° C; at this temperature, a dehalogenation process starts. The dehalogenation enthalpies and peak temperatures are given in Table 3. In general, these

TABLE 2

IR data (cm^{-1}) for $PdBr_2(LH)_2$ complexes

Compound	ν(O–H)	ν(N–H)	$\nu(C_2=O)$	$\nu(C_6=O)$	ν(C=C) + ν(C=N)	ν(Pd–N)	ν(Pd–Br)
$PdBr_2(8EH)_2$	–	3170, 3030	1720 [a]		1575, 1535	265	– [b]
$PdBr_2(1MEH)_2 \cdot H_2O$	3560	3165, 3090	1725	1670	1585, 1535	265	– [b]
$PdBr_2(TBH)_2$	–	3142	1708	1690	1596, 1555	254	237
$PdBr_2(DMH)_2 \cdot 3H_2O$	3460	3180, 3045	1690 [a]		1570, 1535	265	230
$PdBr_2(TFH)_2 \cdot H_2O$	3500 [a]	3125	1700	1650	1530 [a]	255	– [b]
$PdBr_2(CF)_2$	–	–	1711	1660	1607, 1550	– [b]	– [b]
$PdBr_2(TMH)_2 \cdot 2H_2O$	3387	3100	1709	1659	1568, 1544	250	228
$PdBr_2(ETH)_2 \cdot 2H_2O$	3440	3155	1700	1660	1560, 1540	– [b]	225
$PdBr_2(PRH)_2$	–	3115	1704	1669	1561, 1524	– [b]	233
$PdBr_2(IPH)_2$	–	3157	1705	1670	1554, 1522	252	228
$PdBr_2(PH)_2$	–	3140	1720	1670	1560, 1515	– [b]	220

[a] Broad band.

[b] Not observed.

TABLE 3

TG and DSC data for yellow complexes[a]

Compound	Dehydration				Dehalogenation		Pyrolysis		
	%H_2O	ΔT, TG (°C)	T, DSC (°C)	ΔH (kJ mol^{-1})	T, DSC (°C)	ΔH (kJ mol^{-1})	T_f, TG (°C)	%Δp	T(exo) (°C)
$PdBr_2(8EH)_2$	–	–	–	–	–[c]	–[c]	600	80.2 (80.45)	395, 480
$PdBr_2(1MEH)_2 \cdot H_2O$	3.4 (2.68)	50–120	73	62	330	–[c]	700	83.2 (81.79)	360, 450
$PdBr_2(TBH)_2$	–	–	–	–	376	216	600	80.4 (80.70)	430, 450
$PdBr_2(DMH)_2 \cdot 3H_2O$	8.6 (7.94)	50–175	78, 159	83	355	131	650	81.4 (82.01)	410, 430
$PdBr_2(TFH)_2 \cdot H_2O$	5.7 (5.43)	50–100	76	56	–[c]	–[c]	550	80.6 (81.52)	304, 400, 480, 500
$PdBr_2(CF)_2$	–	–	–	–	318, 332	148[b]	675	81.4 (81.29)	500
$PdBr_2(TMH)_2 \cdot 2H_2O$	5.1 (5.22)	50–95	70, 85	76[b]	393	–[c]	550	82.2 (82.27)	430
$PdBr_2(ETH)_2 \cdot 2H_2O$	5.6 (5.01)	50–130	109	92	342	243	700	82.7 (82.96)	454
$PdBr_2(PRH)_2$	–	–	–	–	322, 325	218[b]	600	82.0 (82.76)	460, 480
$PdBr_2(IPH)_2$	–	–	–	–	336	245	600	82.4 (82.76)	460
$PdBr_2(PH)_2$	–	–	–	–	327	183	650	83.8 (84.03)	380

[a] Calculated values are given in parentheses.

[b] Average integration.

[c] Overlapping with exothermic effects.

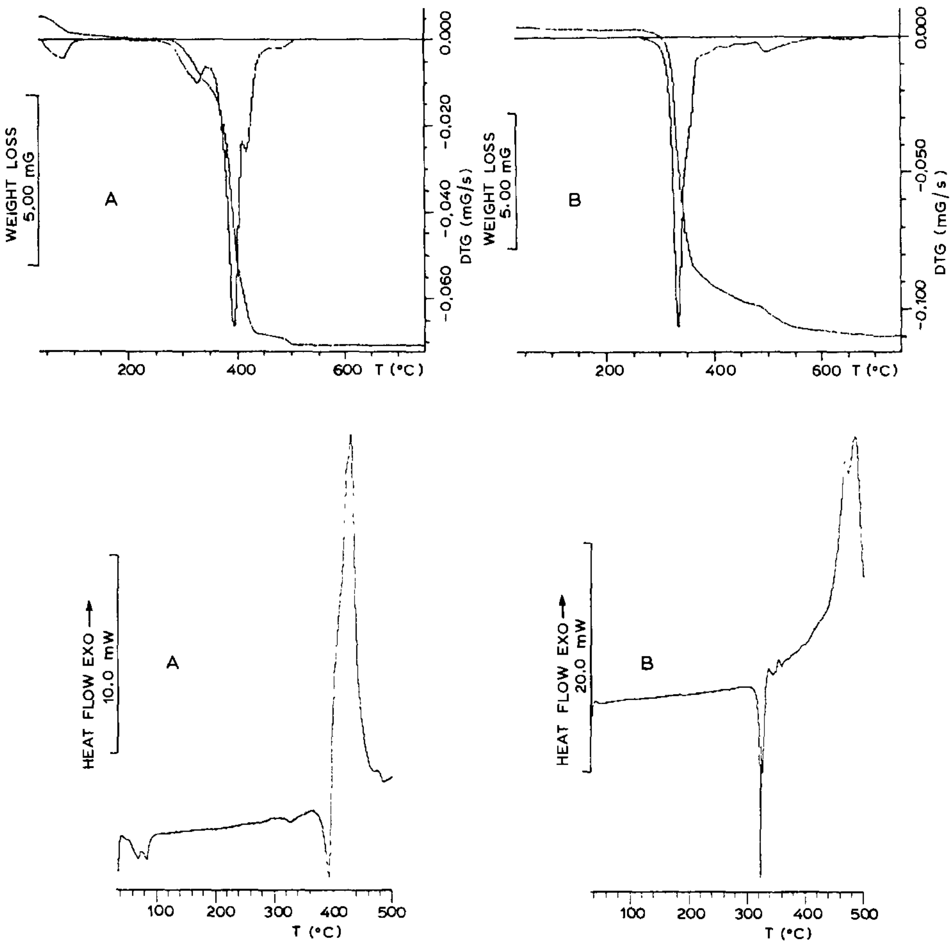

Fig. 1. TG and DSC curves for (A) $PdBr_2(TMH)_2 \cdot 2H_2O$ and (B) $PdBr_2(PRH)_2$.

dehalogenation processes take place at a higher temperature than for the analogous $PdCl_2(LH)_2$ complexes [9,16]. This fact is probably due to the higher capacity of bromine ligand, with respect to chlorine ligand, to establish a π bond with the metal ion by retrodonation.

The dehalogenated compounds are not stable and rapidly start to decompose. These decompositions appear in the DSC curves as exothermic effects the temperature peaks of which are given in Table 3. In all cases, PdO was obtained as the final product of the pyrolysis. The experimental and calculated weight losses are also shown in Table 3.

Red complexes

Spectral studies carried out on these compounds have shown that they are all salts containing the corresponding xanthine derivative in monoproto-

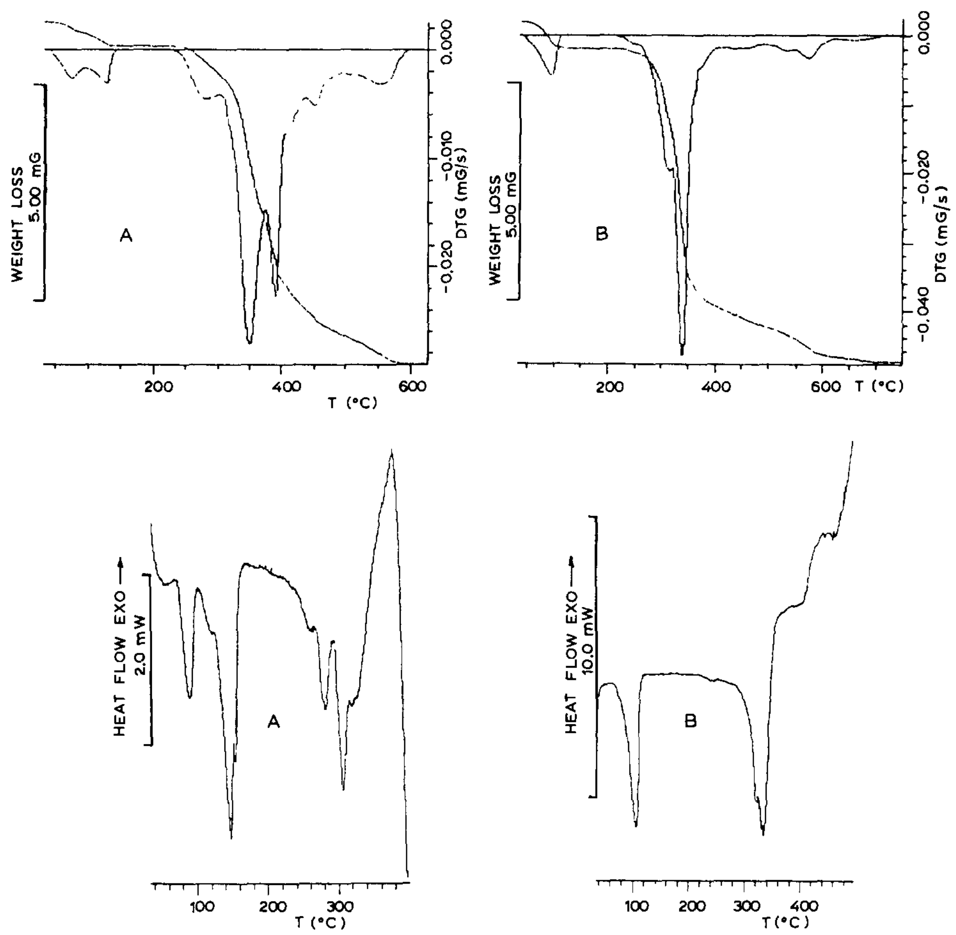

Fig. 2. TG and DSC curves for (A) $PdBr_3(TMH_2)\cdot H_2O$ and (B) $PdBr_3(PRH_2)\cdot 2H_2O$.

nated form as a cation [13]. On the other hand, X-ray studies carried out on the $[PdBr_3][TMH_2]\cdot H_2O$ ligand [13] indicate that the unit cell consists of dinuclear $[Pd_2Br_6]^{2-}$ anions, containing two bridging bromine ligands and trimethylxanthinium cations in which hydrogen atoms are bound to both imidazolic nitrogen atoms.

On heating these compounds three processes can occur: dehydration, dehalogenation and pyrolitic decomposition. These have been discerned and studied from the corresponding TG and DSC curves; those corresponding to $[PdBr_3][TMH_2]\cdot H_2O$ and $[PdBr_3][PRH_2]\cdot 2H_2O$ are given in Fig. 2.

Dehydration processes

With the exception of $[PdBr_4][TBH_2]_2$ and $[PdBr_4][TFH_2]_2$, the first step

TABLE 4

TG and DSC data for red complexes [a]

Compound	Dehydration				Dehalogenation		Pyrolysis		
	%H_2O	ΔT, TG (°C)	T, DSC (°C)	ΔH (kJ mol^{-1})	T, DSC (°C)	ΔH (kJ mol^{-1})	T_f, TG (°C)	%Δp	T(exo) (°C)
$PdBr_4(TBH_2)_2$	–	–	–	–	320, 363	136, 51	650	85.2 (84.47)	> 500
$PdBr_4(TFH_2)_2$	–	–	–	–	327	186	575	84.7 (84.47)	> 500
$PdBr_3(CFH)\cdot 7H_2O$	19.2 (18.35)	50–150	67, 116	74, 102	292, 305	113 [b]	650	80.8 (81.65)	420
$PdBr_3(TMH_2)\cdot H_2O$	3.1 (3.22)	100–165	148, 151	59	280, 300	– [c]	600	78.8 (78.11)	380
$PdBr_3(ETH_2)\cdot H_2O$	3.6 (3.14)	60–140	70, 95, 128	68 [b]	296, 336	39, 181	650	78.9 (78.65)	> 400
$PdBr_3(PRH_2)\cdot 2H_2O$	6.1 (5.94)	50–120	106	104	363	203	600	80.2 (79.78)	> 500
$PdBr_3(IPH_2)\cdot 2H_2O$	5.7 (5.94)	50–130	70, 100, 125	129 [b]	340, 342	259 [b]	600	80.0 (79.78)	> 500
$PdBr_3(PH_2)\cdot H_2O$	3.5 (2.93)	50–130	98, 105, 120	61 [b]	315, 320	122 [b]	650	82.1 (80.10)	> 500

[a] Calculated values are given in parentheses.

[b] Average integration.

[c] Overlapping with exothermic effects.

of the thermal decomposition of these red compounds is the elimination of water. Thermoanalytic data for these processes are given in Table 4.

Dehydration of these compounds generally occurs in different steps which is in agreement with the experimental results obtained from the X-ray study of $[PdBr_3][TMH_2] \cdot H_2O$ [13]. Weight losses observed in the TG curves are in agreement with those calculated from the corresponding formulae. The expected endothermic behaviour for such processes has been observed in DSC curves in the same temperature range. The corresponding dehydration enthalpies and temperature peaks are given in Table 4. Dehydration enthalpy values are fairly high. This suggests a very strong interaction between water molecules and the corresponding xanthine derivative. In the case of the TMH compound, this interaction is established through three hydrogen bonds, where a water molecule acts as the acceptor for a $N9-H \cdots O(w)$ bond and as the donor toward O2 and Br3 atoms [13].

Dehalogenation processes

Data corresponding to dehalogenation processes are shown in Table 4. Most DSC curves show two endothermic effects for the total dehalogenation of these compounds. Temperature peaks and enthalpy values for these processes are collected in Table 4. The enthalpy values are very similar to those observed for the dehalogenation processes of $PdBr_2(LH)_2$ complexes, which suggests a similar strength of the Pd–Br bonds, in both cases. It is possible to propose from DSC curves that the dehalogenation occurs by loss of HBr and Br_2; this dehalogenation mode has also been suggested for other xanthinium halometallates [10,11] on the basis of IR spectra of the intermediate species [11].

Pyrolytic processes

Once dehalogenated, the red compounds show exothermic effects in their DSC curves, which are attributed to the combustion of organic matter, giving PdO as the final product. Weight losses observed in TG curves are in agreement with those calculated for the theoretical residue. These values are given in Table 4. The resulting PdO residue was identified by IR spectroscopy.

REFERENCES

1 G.L. Eichhorn, in G.L. Eichhorn (Ed.), Inorganic Biochemistry, Elsevier, Amsterdam, 1973, Chaps. 3 and 4.

2 B. Rosenberg, L. Van Camp, J.E. Trosko and V.H. Mansour, Nature (London), 222 (1969) 385.

3 B. Rosenberg and L. Van Camp, Cancer Res., 30 (1970) 1977.
4 P.G. Olafson, A.M. Bryan and K. Lau, J. Therm. Anal., 11 (1977) 377.
5 D.J. Hodgson, Progr. Inorg. Chem., 23 (1977) 211.
6 L.G. Marzilli, Progr. Inorg. Chem., 23 (1977) 255.
7 R.B. Martin, Acc. Chem. Res., 18 (1985) 32.
8 J.M. Salas-Peregrín, E. Colacio-Rodríguez and E. Sánchez-Martínez, Thermochim. Acta, 86 (1985) 189.
9 E. Colacio-Rodríguez, J.M. Salas-Peregrín, J. Ruiz-Sánchez and E. García-Megías, Thermochim. Acta, 89 (1985) 159.
10 E. Colacio-Rodríguez, M.N. Moreno-Carretero and J.M. Salas-Peregrín, J. Therm. Anal., 30 (1985) 771.
11 M.N. Moreno-Carretero, E. Colacio-Rodríguez and J.M. Salas-Peregrín, Thermochim. Acta, 97 (1986) 67, and references therein.
12 J.H. Speer and A. Raymond, J. Am. Chem. Soc., 75 (1953) 114.
13 M.I. Moreno-Vida, E. Colacio-Rodríguez, M.N. Moreno-Carretero, J.M. Salas-Peregrín, M. Simard and A.L. Beauchamp, Inorg. Chim. Acta, submitted.
14 J.M. Salas-Peregrín, E. Sánchez-Martínez and E. Colacio-Rodríguez, Inorg. Chim. Acta, 107 (1985) 23.
15 M.N. Moreno-Carretero, E. Colacio-Rodríguez, J.M. Salas-Peregrín and M.P. Sánchez-Sánchez, An. Quim., 81B (1985) 313.
16 J.M. Salas-Peregrín, E. Colacio-Rodríguez, M.A. Romero-Molina and M.P. Sánchez-Sánchez, Thermochim. Acta, 69 (1983) 313.